CONVENTIONAL MAGNETS – I

Neil Marks.
Daresbury Laboratory, Warrington, UK.

Abstract
The design and construction of conventional, steel-cored, direct-current magnets are discussed. Laplace's equation and the associated cylindrical harmonic solutions in two dimensions are established. The equations are used to define the ideal pole shapes and required excitation for dipole, quadrupole and sextupole magnets. Standard magnet geometries are then considered and criteria determining the coil design are presented. The use of codes for predicting flux density distributions and the iterative techniques used for pole face design are then discussed. This includes a description of the use of two-dimensional codes to generate suitable magnet end geometries. Finally, standard constructional techniques for cores and coils are described.

1. INTRODUCTION

This first paper is restricted to direct current situations, in which voltages generated by the rate of change of flux and the resulting eddy-current effects are negligible. This situation therefore includes slowly varying magnets used to ramp the energy of beams in storage rings, together with the normal effects of energising and de-energising magnets in fixed energy machines.

Formally, the term 'field' refers to the magneto-motive force in a magnetic circuit, expressed in Amps/metre and for which the conventional symbol is **H**. In a medium or free space this generates a magnetic flux (units Webers, symbol Φ). The flux per unit cross section is referred to as either the 'flux density' or the 'induction'; this has units of Tesla (T) and symbol **B**. Students new to the topic may well be confused by the almost universal habit, in conversations involving accelerator and magnet practitioners, of referring to 'flux density' also as 'field'. This can be justified by the identical nature of the distributions of the two quantities in areas of constant permeability and, particularly, in free space. This, of course, is not the case for the units of the two quantities. Hence, when distributions only are being referred to, this paper will also use the term field for both quantities. Further difficulties may arise due to the use of the old unit Gauss (and Kilo-Gauss) as the unit of flux density ($1T = 10^4$ G) in some computer codes.

2 MAGNETO-STATIC THEORY

2.1 Allowed Flux Density Distributions in Two Dimensions.

A summary of the conventional text-book theory for the solution of the magneto-static equations in two dimension is presented in Box 1. This commences with the two Maxwell equations that are relevant to magneto-statics:

div **B**=0

curl **H** =**j**

The assumption is made, at this stage, that electric currents are not present in the immediate region of the problem and hence **j**, the vector current density, is zero. The fuller significance of this will appear later; it does not imply that currents are absent throughout all space.

With the curl of the magnetic field equal to zero, it is then valid to express the induction as the gradient of a scalar function Φ, known as the magnetic scalar potential. Combining this with the divergence equation gives the well known Laplace's equation.

The problem is then limited to two dimensions and the solution for the scalar potential in polar coordinates (r, θ) for Laplace's equation is given in terms of constants E, F, G, and H, an integer n, and an infinite series with constants J_n, K_n, L_n and N_n. The terms in (ln r) and in r^{-n} in the summation all become infinite as r tends to zero, so in practical situations the coefficients of these terms are zero. Likewise, the term in θ is many valued, so F can also be set to zero.

This gives a set of cylindrical harmonic solutions for Φ expressed in terms of the integer n and and two associated constants J_n and K_n. It will be seen that these are determined from the geometry of the magnet design. By considering the grad of Φ, equations for the components of the flux density (B_r and B_θ) are obtained as functions of r and θ.

Maxwell's equations for magneto-statics:

$$.\mathbf{B} = 0 ;$$
$$\langle \mathbf{H} = \mathbf{j} ;$$

In the absence of currents:

$$\mathbf{j} = 0.$$

Then we can put:

$$\mathbf{B} = \quad \Phi$$

so that:

$$^2\Phi = 0 \quad \text{(Laplace's equation)}$$

where Φ is the magnetic scalar potential.

Taking the two dimensional case (constant in the z direction) and solving for coordinates (r,θ):

$$\Phi = (E+F\theta)(G+H \ln r) \quad {}_{n=1}{}^{\times} (J_n r^n \cos n\theta + K_n r^n \sin n\theta + L_n r^{-n} \cos n\theta + M_n r^{-n} \sin n\theta)$$

In practical magnetic applications, this becomes:

$$\Phi = \quad {}_n (J_n r^n \cos n\theta + K_n r^n \sin n\theta),$$

with n integral and J_n,K_n a function of geometry.

This gives components of flux density:

$$B_r = \quad {}_n (n J_n r^{n-1} \cos n\theta + nK_n r^{n-1} \sin n\theta)$$
$$B_\theta = \quad {}_n (-nJ_n r^{n-1} \sin n\theta + nK_n r^{n-1} \cos n\theta)$$

Box 1: Magnetic spherical harmonics derived from Maxwell's equations.

It must be stressed that all possible physical distributions of flux density in two dimensions are described by these equations. For a particular value of n, there are two degrees of freedom given by the magnitudes of the corresponding values of J and K; in general these connect the distributions in the two planes. Hence, once the values of the two constants are defined, the

distributions **in both planes** are also defined. Behaviour in the vertical plane is determined by the distribution in the horizontal plane and vice versa; they are not independent of each other. The practical significance of this is that, provided the designer is confident of satisfying certain symmetry conditions (see later section), it is not necessary to be concerned with the design or the measurement of magnets in the two transverse dimensions; a one-dimensional examination will usually be sufficient.

The condition relating to the presence of currents can now be defined in terms of the polar coordinates. The solution for Φ in Box 1 is valid providing currents are absent within the range of r and θ under consideration. In practical situations, this means areas containing free space and current-free ferro-magnetic material, up to but excluding the surfaces of current-carrying conductors, can be considered.

2.2 Dipole, Quadrupole and Sextupole Magnets

Each value of the integer n in the magnetostatic equations corresponds to a different flux distribution generated by different magnet geometries. The three lowest values, n=1, 2, and 3 correspond to dipole, quadrupole and sextupoles flux density distributions respectively; this is made clearer in Boxes 2, 3 and 4. In each case the solutions in Cartesian coordinates are also shown, obtained from the simple transformations:

$$B_x = B_r \cos\theta - B_\theta \sin\theta,$$
$$B_y = B_r \sin\theta + B_\theta \cos\theta.$$

For the **dipole field** (Box 2), the lines of equipotential, for the J=0, K non-zero case, are equispaced and parallel to the x axis. The gradient gives a constant vertical field; if J were zero, the lines of **B** would be horizontal. This therefore is a simple, constant magnetic distribution combining vertical and horizontal flux densities, according to the values of J and K and is the common magnetic distribution used for bending magnets in accelerators.

Note that we have not yet addressed the conditions necessary to obtain such a distribution.

Cylindrical:	**Cartesian:**
$B_r = J_1 \cos\theta + K_1 \sin\theta;$	$B_x = J_1$
$B_\theta = -J_1 \sin\theta + K_1 \cos\theta;$	$B_y = K_1$
$\Phi = J_1 r \cos\theta + K_1 r \sin\theta.$	$\Phi = J_1 x + K_1 y$

So, $J_1 = 0$, $K_1 \neq 0$ gives vertical dipole field:

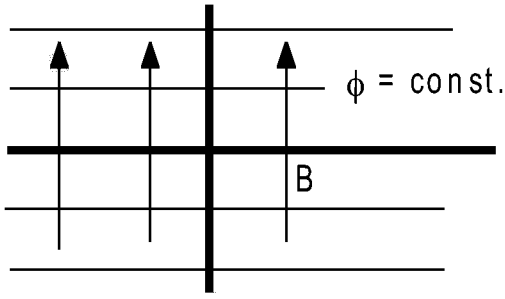

$K_1 = 0$, $J_1 \neq 0$ gives horizontal dipole field.

Box 2: Dipole field given by n=1 case.

Cylindrical:

$B_r = 2 J_2 r \cos 2\theta + 2K_2 r \sin 2\theta;$
$B_\theta = -2J_2 r \sin 2\theta + 2K_2 r \cos 2\theta;$
$\Phi = J_2 r^2 \cos 2\theta + K_2 r^2 \sin 2\theta;$

Cartesian:

$B_x = 2 (J_2 x + K_2 y)$
$B_Y = 2 (-J_2 y + K_2 x)$
$\Phi = J_2 (x^2 - y^2) + 2K_2 xy$

These are quadrupole distributions, with $J_2 = 0$ giving 'normal' quadrupole field.

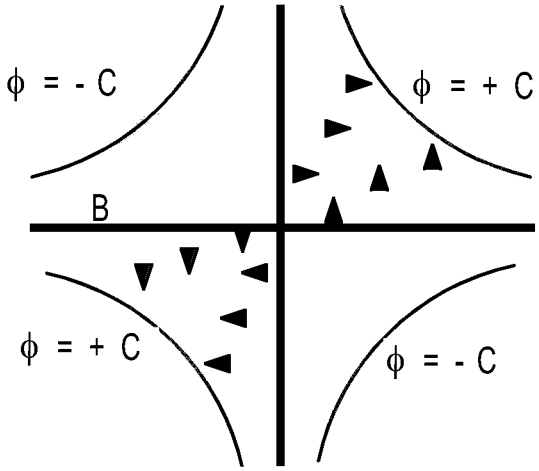

Then $K_2 = 0$ gives 'skew' quadrupole fields (which is the above rotated by $\pi/4$).

Box 3: Quadrupole field given by n=2 case.

For the n=2 case (Box 3) the **quadrupole field** is generated by lines of equipotential having hyperbolic form. For the J=0 case, the asymptotes are the two major axes and the flux distributions are normal to the axes at the axes; the amplitudes of the horizontal and vertical components vary linearly with the displacements from the origin. With zero induction in both planes at the origin, this distribution provides linear focusing of particles. As explained in the paper on linear optics, a magnet that is focusing in one plane will defocus in the other. This is an important example of the point explained above; the distributions in the two planes cannot be made independent of each other.

The J=0 case dealt with above is described as the normal quadrupole field. For zero value of the constant K (non-zero J) the situation is rotated by $\pi/4$ and the distribution is referred to as a skew quadrupole field.

The equations for **sextupole field** distribution are given in Box 4. Again, the normal sextupole distribution corresponds to the J=0 case. Note the lines of equipotential with six-fold symmetry and the square law dependency of the vertical component of flux density with horizontal position on the x axis. As explained in the papers dealing with particle optics, normal sextupole field is used to control chromaticity - the variation in focusing with particle momentum.

Cylindrical :

$B_r = 3 J_3 r^2 \cos 3\theta + 3K_3 r^2 \sin 3\theta;$
$B_\theta = -3 J_3 r^2 \sin 3\theta + 3K_3 r^2 \cos 3\theta;$
$\Phi = J_3 r^3 \cos 3\theta + K_3 r^3 \sin 3\theta;$

Cartesian:

$B_x = 3 J_3 (x^2 - y^2) + 6K_3 xy$
$B_y = -6J_3 xy + 3K_3 (x^2 - y^2)$
$\Phi = J_3 (x^3 - 3y^2x) + K_3 (3yx^2 - y^3)$

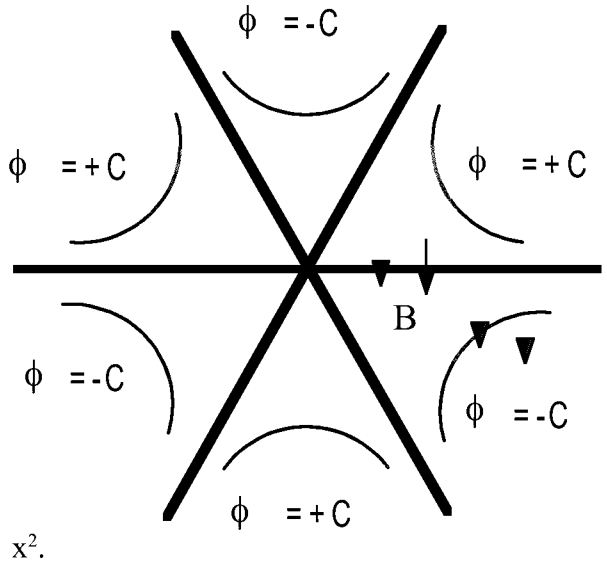

For $J_3 = 0$, $B_y \quad x^2$.

Box 4: Sextupole field given by n=3 case.

The sextupole skew field case is given by K=0, (J non-zero), and is rotated by $\pi/6$.

It is now clear that ascending powers of n give higher orders of field harmonics, the circular symmetry having the order of 2n. It is easy to show that for any n, the vertical component of flux density on the x axis for a 'normal' distribution is proportional to x to the power (n-1):

$$B_y (y=0) \quad x^{n-1}$$

It must be stressed that in spite of reference to practical magnetic situations, the treatment of each harmonic separately is still a mathematical abstraction. Whilst the designer may strive to produce a magnet generating only one type of field, in practical situations many harmonics will be present and many of the coefficients J_n and K_n will be non-zero. A successful design will, however, minimise the unwanted terms (particularly the skew terms in a normal magnet) to small values.

In some cases the magnet is designed to produce more than one type of field and multiple harmonics are required. A classic example is the combined-function bending magnet, which includes dipole and quadrupole field at the beam position. The different harmonic fields are generated by the shaping of the pole and the ratio between the dipole and quadrupole components is therefore fixed by this geometry; such a magnet can be regarded as a conventional quadrupole with the origin shifted to provide non-zero induction at the magnet's centre. More recently, the

criticality of space in accelerator lattices has led to the investigation of geometries capable of generating dipole, quadrupole and sextupole field in the same magnet, with independent control of the harmonic amplitudes, and a number of successful designs have been produced.

2.3 Ideal Pole Shapes

To the basic theoretical concepts of the field harmonics, we shall now add the more practical issue of the ferro-magnetic surfaces required to make up the magnet poles. To many, it is intuitively obvious that the correct pole shape to generate a particular harmonic, for the ideal case of infinite permeability, is a line of constant scalar potential. This is explained more fully in Box 5. This is the standard text book presentation for proving that flux lines are normal to a surface of very high permeability; it then follows from the definition:

$$\mathbf{B} = \text{grad } \Phi$$

that this is also an equi-potential line.

The resulting ideal pole shapes for (normal) dipole, quadrupole and sextupole magnets are then given in Box 6. These are obtained from the Cartesian equipotential equations with the J coefficients set to zero, and geometric terms substituted for K. For perfect, singular harmonics, infinite poles of the correct form, made from infinite permeability steel with currents of the correct

At the steel boundary, with no currents in the steel:

$$\text{curl } \mathbf{H} = 0$$

Apply Stoke's theorem to a closed loop enclosing the boundary:

$$(\text{curl } \mathbf{H}).d\mathbf{S} = \mathbf{H}.d\mathbf{s}$$

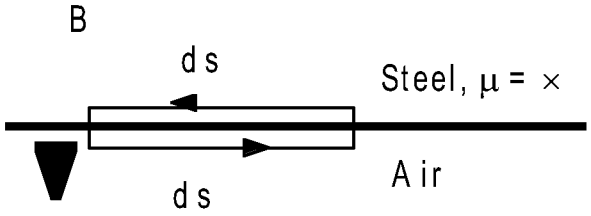

Hence around the loop: $\mathbf{H}.\,d\mathbf{s} = 0$

But for infinite permeability in the steel: $\mathbf{H}=0$;

Therefore outside the steel $\mathbf{H}=0$ parallel to the boundary.

Therefore **B** in the air adjacent to the steel is normal to the steel surface at all points on the surface.

Therefore from $\mathbf{B}=\text{grad } \Phi$, the steel surface is an iso-scalar-potential line.

Box 5: Ideal pole shapes are lines of equal magnetic

For normal (ie not skew) fields:

Dipole:

$y = \angle g/2$;

(g is interpole gap).

Quadrupole:

$xy = \angle R^2/2$;

(R is inscribed radius).

Sextupole:

$3x^2y - y^3 = \angle R^3$;

Box 6: Equations of ideal pole shape

Magnet	Symmetry	Constraint
Dipole	$\phi(\theta) = -\phi(2\pi - \theta)$	All $J_n = 0$;
	$\phi(\theta) = \phi(\pi - \theta)$	K_n non-zero only for: n = 1, 3, 5, etc;
Quadrupole	$\phi(\theta) = -\phi(\pi - \theta)$	$K_n = 0$ for all odd n;
	$\phi(\theta) = -\phi(2\pi - \theta)$	All $J_n = 0$;
	$\phi(\theta) = \phi(\pi/2 - \theta)$	K_n non-zero only for: n = 2, 6, 10, etc;
Sextupole.	$\phi(\theta) = -\phi(2\pi/3 - \theta)$	$K_n = 0$ for all n not
	$\phi(\theta) = -\phi(4\pi/3 - \theta)$	multiples of 3;
	$\phi(\theta) = -\phi(2\pi - \theta)$	All $J_n = 0$;
	$\phi(\theta) = \phi(\pi/3 - \theta)$	K_n non-zero only for: n = 3, 9, 15, etc.

Box 7: Symmetry constraints in normal dipole, quadrupole and sextupole geometries.

magnitude and polarity located at infinity are sufficient; in practical situations they are happily not necessary. It is possible to come close to the criterion relating to the steel permeability, for values of μ in the many thousands are possible, and the infinite permeability approximation gives good results in practical situations. Various methods are available to overcome the necessary finite sizes of practical poles and certain combinations of conductor close to high-permeability steel produce good distributions up to the surface of the conductors. Before examining such 'tricks', we shall first investigate the theoretical consequences of terminating the pole according to a practical geometry.

2.4 Symmetry Constraints

The magnet designer will use the ideal pole shapes of Box 6 in the centre regions of the pole profile, but will terminate the pole with some finite width. In so doing, certain symmetries will be imposed on the magnet geometry and these in turn will constrain the harmonics that can be present in the flux distribution generated by the magnet. The situation is defined in a more mathematical manner in Box 7.

In the case of the normal, vertical field dipole, the designer will place two poles equi-distant from the horizontal centre line of the magnet; these will have equal magnitude but opposite polarity of scalar potential. This first criterion ensures that the values of J_n are zero for all n. Providing the designer ensures that the pole 'cut-offs' of both the upper and lower pole are symmetrical about the magnet's vertical centre line, the second symmetry constraint will ensure that

all K_n values are zero for even n. Thus, with two simple symmetry criteria, the designer has ensured that the error fields that can be present in the dipole are limited to sextupole, decapole, fourteen-pole, etc.

In the case of the quadrupole, the basic four-fold symmetry about the horizontal and vertical axes (the first two criteria) render all values of J_n and the values of K_n for all odd n equal to zero. The third constraint concerns the eight-fold symmetry ie the pole cut-offs being symmetrical about the $\pi/4$ axes. This makes all values of K_n zero, with the exception of the coefficients that correspond to n=2 (fundamental quadrupole), 6, 10, etc. Thus in a fully symmetric quadrupole magnet, the lowest-order allowed field error is twelve pole (duodecapole), followed by twenty pole, etc.

Box 7 also defines the allowed error harmonics in a sextupole and shows that with the basic sextupole symmetry, eighteen pole is the lowest allowed harmonic error; the next is thirty pole. Higher order field errors are therefore usually not of high priority in the design of a sextupole magnet.

Given the above limitations on the possible error fields that can be present in a magnet, the magnet designer has additional techniques that can be used to reduce further the errors in the distribution; these usually take the form of small adjustments to the pole profile close to the cut-off points.

It must be appreciated that the symmetry constraints described in this section apply to magnet geometries as designed. Construction should closely follow the design but small tolerance errors will always be present in the magnet when it is finally assembled and these will break the symmetries described above. Thus, a physical magnet will have non-zero values of all J and K coefficients. It is the task of the magnet engineer to predict the distortions resulting from manufacturing and assembly tolerances; this information then becomes the basis for the specification covering the magnet manufacture, so ensuring that the completed magnet will meet its design criteria.

Before leaving the topic of magnetic cylindrical harmonics, it is necessary to put this concept into the wider context of the interaction of beams with magnetic fields. Particles are not able to carry out a cylindrical harmonic analysis and are therefore not sensitive to the amplitude or phase of a particular harmonic in a magnet. They see flux densities **B** and, in resonance type phenomena, the spatial differentials of **B**, sometimes to high orders. It is a mistake, therefore, to associate a certain order of differential with one particular harmonic, as all the higher harmonic terms will contribute to the derivative; the magnet designer may well have balanced the amplitudes and polarities of a number of quite high harmonics to meet successfully a stringent flux density criterion within the defined good field region of the magnet.

The two-dimensional cylindrical harmonics are therefore a useful theoretical tool and give a valuable insight into the allowed spatial distributions of magnetic fields. However, when judging the viability of a design or the measurements from a completed magnet, always re-assemble the harmonic series and examine the flux density or its derivatives. These are the quantities corresponding to the physical situation in an accelerator magnet.

3 PRACTICAL ASPECTS OF MAGNET DESIGN

3.1 Coil Requirements

Current-carrying conductors will now be added to the consideration of magnet design. Central to this development is the equation:

$$\text{curl } \mathbf{H} = \mathbf{j},$$

and the application of the well known Stoke's theorem to the magnetic circuit. This is summarised in Box 8. This shows the transformation of the vector equation into the scalar relationship equating the line integral of the field **H** to the area integral of the enclose current density **j**. The resulting equation is fundamental to all electromagnetic applications.

The application of this to a simple dipole circuit with a high permeability ferromagnetic core is shown in Box 9. This demonstrates how, with approximately constant flux density **B** around the complete circuit, the Ampere-turns are concentrated across the gap g. This gives the required Ampere-turns in a dipole circuit. The expression, relating the flux density to the magneto-motive force and the magnet dimensions is roughly analogous to the simple expression for current in an electrical circuit containing an emf and resistance. The similarity is strengthened by the nomenclature that refers to the terms 'g' and 'ℓ/μ' as the reluctance of the gap and the steel core respectively.

In Box 10, one method for establishing the required Ampere-turns per pole for quadrupole and sextupole magnets is shown. The method can be applied generally to higher-order multipole magnets.Note that the strength of the quadrupole in Box 10 is defined in terms of the 'gradient'. In the case of the quadrupole, this is unambiguous, for if

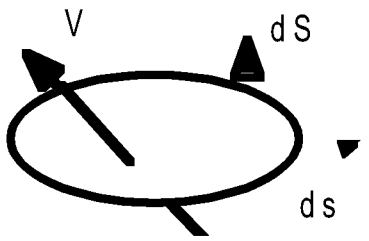

Stoke's theorem for vector **V**:

V.ds = **curl V.dS**

Apply this to:

curl H = **j**;

Then for any magnetic circuit:

H.ds = NI;

NI is total Amp-turns through loop **dS**.

Box 8: Magneto-motive force in a magnetic circuit.

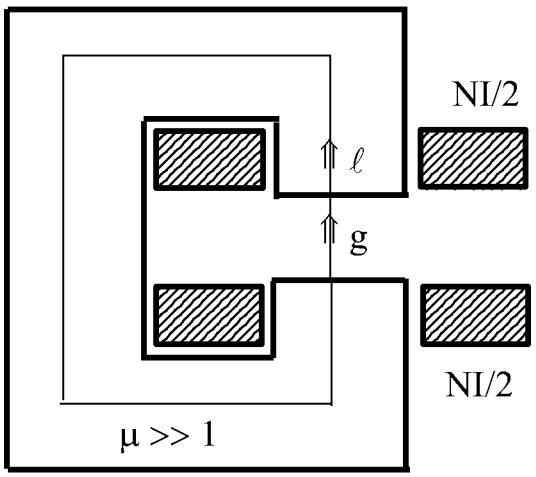

B is approx constant round loop ℓ & g,

and $\mathbf{H}_{iron} = \mathbf{H}_{air}/\mu$;

$\mathbf{B}_{air} = \mu_0 \, NI / (g + \ell/\mu)$;

g, and ℓ/μ are the 'reluctance' of the gap and the iron.

Ignoring iron reluctance:

$NI = \mathbf{B}\, g / \mu_0$

Box 9: Ampere-turns in a dipole.

the field is expressed as:

$$B_y = gx$$

where g is the quadrupole gradient, then

$$dB_y/dx = g$$

ie, g is both the field coefficient and the magnitude of the first derivative. For a sextupole, the second differential is twice the corresponding coefficient:

$$B_y = g_S\, x^2$$

$$d^2B_y/dx^2 = 2\, g_S$$

In the case of sextupoles and higher order fields, it is therefore essential to state whether the coefficient or the derivative is being defined.

Quadruple has pole equation:

$$xy = R^2/2.$$

On x axes

$$B_y = gx,$$

g is gradient (T/m).

At large x (to give vertical **B**):

$$NI = (gx)\,(R^2/2x)/\mu_0$$

ie

$$NI = g\,R^2/2\,\mu_0 \quad \text{(per pole)}$$

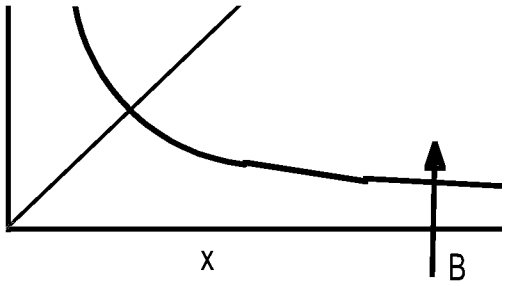

Similarly, for a sextupole, (field coefficient g_S), excitation per pole is:

$$NI = g_S\,R^3/3\,\mu_0$$

Box 10: Ampere-turns in quadrupole and sextupole.

3.2 Standard Magnet Geometries

A number of standard dipole magnet geometries are described in Box 11. The first diagram shows a '**C-core**' magnet. The coils are mounted around the upper and lower poles and there is a single asymmetric backleg. In principal, this asymmetry breaks the standard dipole symmetry described in section 2.4 but, providing the core has high permeability, the resulting field errors will be small. However, a quadrupole term will normally be present, resulting in a gradient of the order of 0.1% across the pole. As this will depend on the permeability in the core, it will be non-linear and vary with the strength of the magnet.

To ensure good quality dipole field across the required aperture, it is necessary to compensate for the finite pole width by adding small steps at the outer ends of each of the pole; these are called shims. The designer must optimise the shim geometry to meet the field distribution requirements. The maximum flux density across the pole face occurs at these positions, and as the shims project above the face, it is essential to ensure that their compensating effect is present at all specified levels of magnet operation. Some designers prefer to make the poles totally flat, resulting in a considerable increase in required pole width to produce the same extent of good field that would be achieved by using shims. Non-linear effects will still be present, but these will not be as pronounced as in a shimmed pole.

The C-core represents the standard design for the accelerator dipole magnet. It is straight

'C' Core:

Advantages:
- Easy access;
- Classic design;

Disadvantages:
- Pole shims needed;
- Asymmetric (small);
- Less rigid;

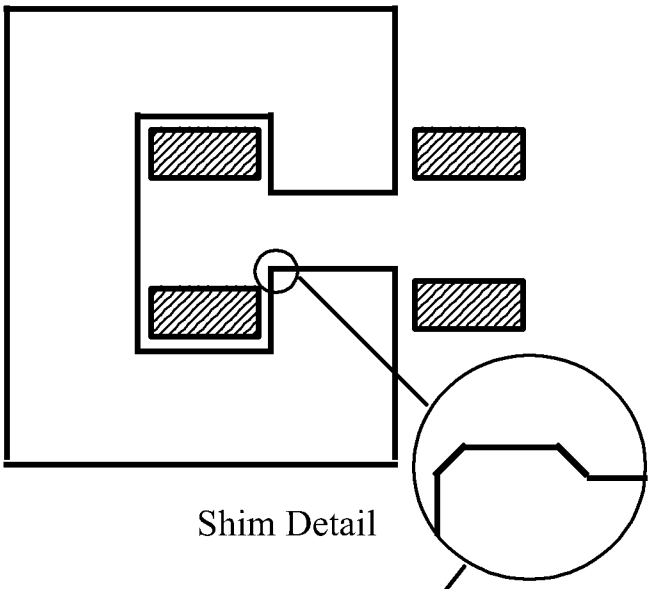

'H' Type

Advantages:
- Symmetric;
- More rigid;

Disadvantages:
- Also needs shims;
- Access problems.

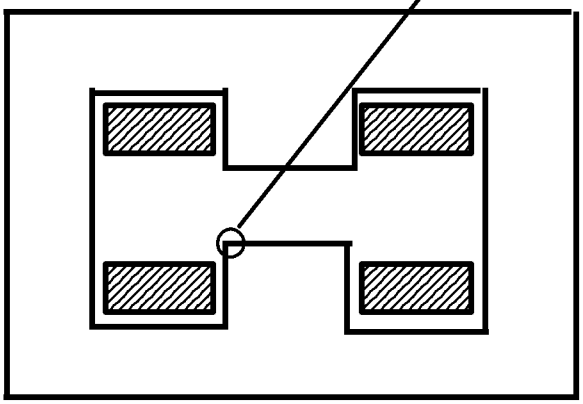

'Window Frame'

Advantages:
- No pole shim;
- Symmetric;
- Compact;
- Rigid;

Disadvantages:
- Major access problems;
- Insulation thickness.

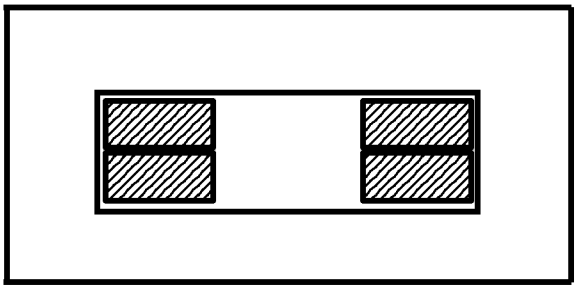

Box 11: Dipole goemetries, with advantages and disadvantages.

forward to manufacture and provides good access to the vacuum vessel and other beam-line components.

The '**H-type**' dipole is very similar to the C core, but has two return backlegs, making the magnet fully symmetrical. Quadrupole error fields are therefore eliminated at the expense of restricting access to the pole area. To allow such access, and to mount the coils during magnet assembly, it is necessary to split the magnet at the horizontal median plane. Note that pole shims are still required for this design.

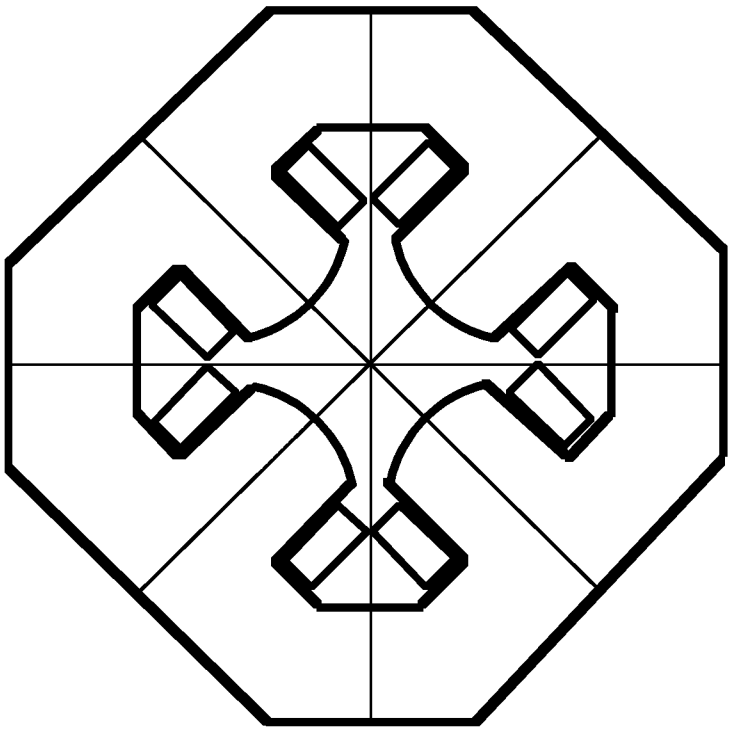

Box 12: Standard quadrupole magnet geometry

The third design is referred to as a '**Window-Frame**' magnet. This is a very compact, rigid design in which the coils are placed on either side of the gap. This has the major advantage of significantly improving the dipole field distribution. Providing the copper conductor extends very closely to the pole, the linearity of exciting Ampere-turns across the gap matches the uniform distribution of the scalar potential in this region, and good field will be achieved right up to the surface of the conductor. In practical situations, the coil insulation takes up a finite space and the good field region is reduced. However, the window frame design has valuable advantages and a number of accelerators have used this concept. There are, however, major access problems.

Box 12 shows a standard design for the quadrupole magnet geometry. The core is symmetric around the four poles, with the coils mounted on the pole sides. This is the equivalent of the H dipole design and shims are required to compensate for the finite pole width. A design corresponding to the window-frame dipole would have the coils on the vertical and horizontal axes, fitting tightly between the extended pole surfaces. This produces good quality field, but provides difficulties in the coil design. In this arrangement, the pole sides diverge by an angle of 90 from the pole face, and the design is therefore suitable for a high gradient quadrupole, where saturation in the pole root could be a problem.

Other variations on the basic quadrupole scheme include a single-sided yoke design, corresponding to the C-cored dipole. This is frequently used in synchrotron radiation sources, where radiation emerges close to the centre of the quadrupole and space is required for a beam pipe in an area that would normally house the outer return yoke.

3.3 Coil Design

The standard coil design uses copper (or occasionally aluminium) conductor with a rectangular cross section. Usually, water cooling (low conductivity de-mineralised water) will be required and in d.c magnets this is achieved by having a circular or racetrack-shaped water channel in the centre of the conductor. The coil is insulated by glass cloth and encapsulated in epoxy resin.

The main tasks in coil design are determining the optimum total cross section of conductor in the coil and deciding on the number of individual turns into which this should be divided.

The factors determining the choice of current density and hence copper cross section area are described in Box 13. Unlike the other criteria that have been examined in earlier parts of this paper, the prime consideration determining conductor area is economic. As the area is increased, the coil, the magnet material and the manufacturing costs increase, whilst the running costs decrease. The designer must therefore balance these effects and make a policy based judgement of the number of years over which the magnet capital costs will be 'written off'. The optimum current density is usually in the range of 3 to 5 A/mm^2, though this will depend on the relative cost of electric power to manufacturing costs that are applicable. Note that the attitude of the funding authority to a proposed accelerator's capital and running cost will also have a major influence on the optimisation of the coil.

$$j = NI/A_C$$

where:

j is the current density,
A_C the area of copper in the coil;
NI is the required Amp-turns.

$$E_C = K\,(NI)^2/A_C$$

therefore

$$E_C = (K\,NI)\,j$$

where:

E_C is energy loss in coil,
K is a geometrical constatnt.

Therefore, for constant NI, loss varies as j.

Magnet capital costs (coil & yoke materials, plus assembly, testing and transport) vary as the size of the magnet ie as 1/j.

Total cost of building and running magnet 'amortised' over life of machine is:

$$£ = P + Q/j + R\,j$$

P, Q, R and therefore optimum j depend on design, manufacturer, policy, country, etc.

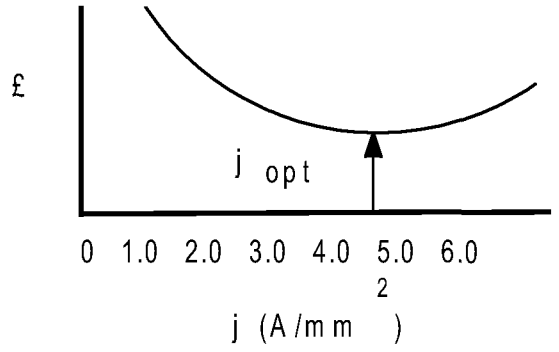

Box 13: Determination of optimum current density in coils.

$I \propto 1/N$, $R_{magnet} \propto N^2 j$, $V_{magnet} \propto N j$, Power $\propto j$

Box 14: Variation of magnet parameters with N and j (fixed NI).

Having determined the total conductor cross section, the designer must decide on the number of turns that are to be used. Box 14 shows how the current and voltage of a coil vary with the current density j and number of turns per coil, N. This leads to the criteria determining the choice of N, as shown in Box 15.

Large N (low current)	**Small N (high current)**
* Small, neat terminals.	* Large, bulky terminals
* Thin interconnections - low cost & flexible.	* Thick, expensive interconnection.
* More insulation layers in coil, hence larger coil, increased assembly costs.	* High percentage of copper in coil. More efficient use of volume.
* High voltage power supply - safety problems.	* High current power supply - greater losses.

Box 15: Factors determining choice of N.

The choice of a small number of turns leads to high currents and bulky terminals and interconnections, but the coil packing factor is high. A large number of turns leads to voltage problems. The optimum depends on type and size of magnet. In a large dipole magnet, currents in excess of 1,000A are usual, whereas smaller magnets, particularly quadrupoles and sextupoles would normally operate with currents of the order of a few hundred Amps. In small corrector magnets, much lower currents may be used and if the designer wishes to avoid the complication of water cooling in such small magnets, solid conductor, rated at a current density of $1A/mm^2$ or less, may be used; the heat from such a coil can usually be dissipated into the air by natural convection.

3.4 Steel Yoke Design

The steel yoke provides the essential ferro-magnetic circuit in a conventional magnet, linking the poles and providing the space for the excitation coils. The gross behaviour of the magnet is determined by the the dimensions of the yoke, for an inadequate cross section will result in excessive flux density, low permeability and hence a significant loss of magneto-motive force (ie Ampere-turns) in the steel. The examination of the properties of steel used in accelerator magnets will be covered in the second conventional magnet paper, which is concerned with a.c. properties. This paper will therefore be restricted to a few general comments relating to yoke design and the significance of coercivity in determining residual fields.

The total flux flowing around the yoke is limited by the reluctance of the air gap and hence the geometry in this region is critical. This is shown in Box 16, indicating that at the gap, in the

transverse plane, the flux extends outwards into a region of fringe field. A rule of thumb used by magnet designers represents this fringe field as extending by one gap dimension on either side of the physical edge of the magnet. This then allows the total flux to be expressed in terms of the pole physical breadth plus the fringe field. Sufficient steel must be provided in the top, bottom and backleg regions to limit the flux density to values that will not allow saturation in the main body of the yoke. Note however that it is usual to have high flux densities in the inside corners at the angles of the yoke. The flux will be distributed so that the reluctance is constant irrespective of the length of the physical path through the steel and this implies that low permeabilities will be encountered in the corners. Providing the region of low permeability does not extend completely across the yoke, this situation is acceptable.

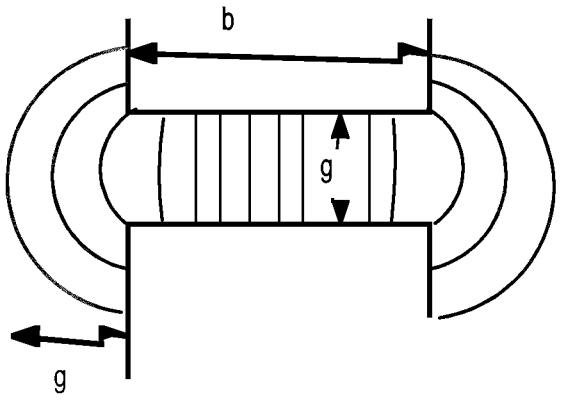

$\Phi \cup B_{gap}$ (b + 2g) l.

Box 16: Flux at magnet gap.

The effect of the gap fringe field has less significance in the longitudinal direction, for this will add to the strength of the magnet seen by the circulating beam; a high fringe field will result in the magnet being run at a slightly lower induction. Thus, the total longitudinal flux is determined by the specified magnetic length and the fringe field in this dimension can be ignored when considering both the flux density in the steel yoke and the inductance in an a.c. magnet.

The yoke will also determine the residual flux density that can be measured in the gap after the magnet has been taken to high field and then had the excitation current reduced to zero. In Box 17 it is explained that the residual field in a gapped magnet is not determined by the 'remanence' or 'remanent field' (as might be ex-

In a continuous ferro-magnetic core, residual field is determined by the remanence B_R. In a magnet with a gap having reluctance much greater than that of the core, the residual field is determined by the coercivity H_C.

With no current in the external coil, the total integral of field H around core and gap is zero.

Thus, if H_g is the field in the gap, ℓ and g are the path lengths in core and gap respectively:

$$ {}_{\ell}H_C \cdot ds + {}_{g}H_g \cdot ds = 0, $$

$$ B_{resid} = - \mu_0 H_C \ell / g $$

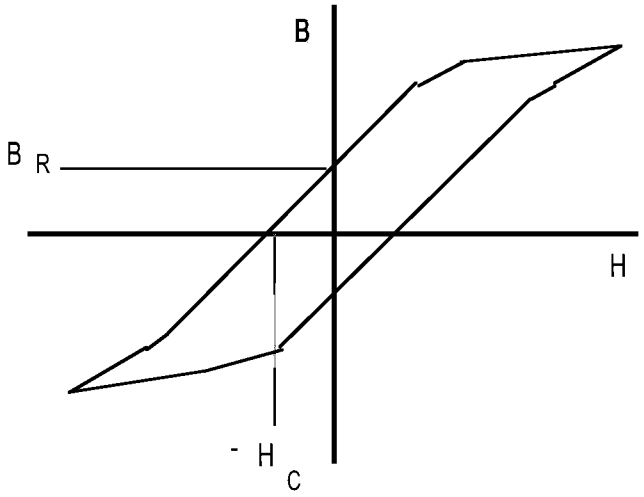

Box 17: Residual field in gapped magnets.

pected from the names given to these parameters) but by the coercive force (in Amps/m) of the hysteresis loop corresponding to the magnetic excursion experienced by the steel. This is because the gap, as previously explained, is the major reluctance in the magnetic circuit and the residual flux density in the gap will be very much less than the remanent field that would be present in an ungapped core. The total Ampere-turns around the circuit are zero and hence the positive field required to drive the residual induction through the gap is equal and opposite to the line integral of (negative) coercive force through the steel.

3.5 Pole face design

Whilst this subject is just a particular feature of the yoke design, it is probably the most vital single feature in the design of an accelerator magnet, for it will determine the field distribution seen by the beam and hence control the behaviour of the accelerator. In the early part of this paper, the various types of field were derived from the cylindrical harmonics and the allowed and forbidden harmonics were established in terms of the magnet's symmetry. It was explained that the remaining error fields, due to there being a non-infinite pole, could then be minimised by the use of shims at the edges of the pole.

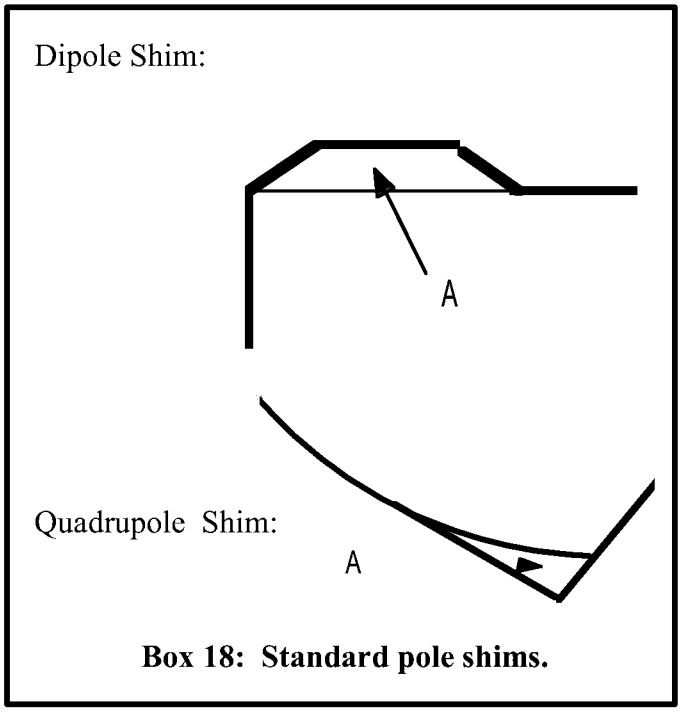

Box 18: Standard pole shims.

Typical shims for dipole and quadrupole magnets are shown in Box 18. The dipole shim takes the form of a trapezoidal extension above the pole face, whilst the quadrupole shim is generated from a tangent to the hyperbolic pole, projecting from some point on the pole face and terminating at the extended pole side.

In both cases, the area A of the shim has the primary influence on the edge correction that is produced. In the dipole case, it is important to limit the height of the shim to prevent saturation in this region at high excitations; this would lead to the field distribution being strongly dependent on the magnet excitation level. On the other hand, if a very low, long shim is used, the nature of the field correction would change, with different harmonics being generated. The shim size and shape is therefore a compromise that depends on the field quality that is desired and on the peak induction in the gap; shim heights and shapes vary widely according to the magnet parameters and the quality of field that is required.

3.6 Pole Calculations

It is the task of the magnet designer to use iterative techniques to establish a pole face that produces a field distribution that meets the field specification: $\Delta B/B$ for a dipole, $\Delta g/g$ for a quadrupole, etc, over a physical 'good-field region'. The main tool in this investigation is one or more computer codes that predict the flux density for a defined magnet geometry; these codes will

be described in the next section. The variables in the optimisation are the width of the pole and the size and shape of the shims. For economy sake (particularly in an a.c.magnet where stored energy determines the power supply rating) the designer will usually wish to minimise the pole width. Having made an initial estimate of a suitable pole width, the magnet designer will explore a range of shims in an attempt to establish a good geometry. If this proves to be impossible, the pole width is increased; if it is easy, economies can possibly be made by reducing the pole width. In this work, past experience is very valuable, and time and trouble is saved by having a rough idea of what will result from a given change.

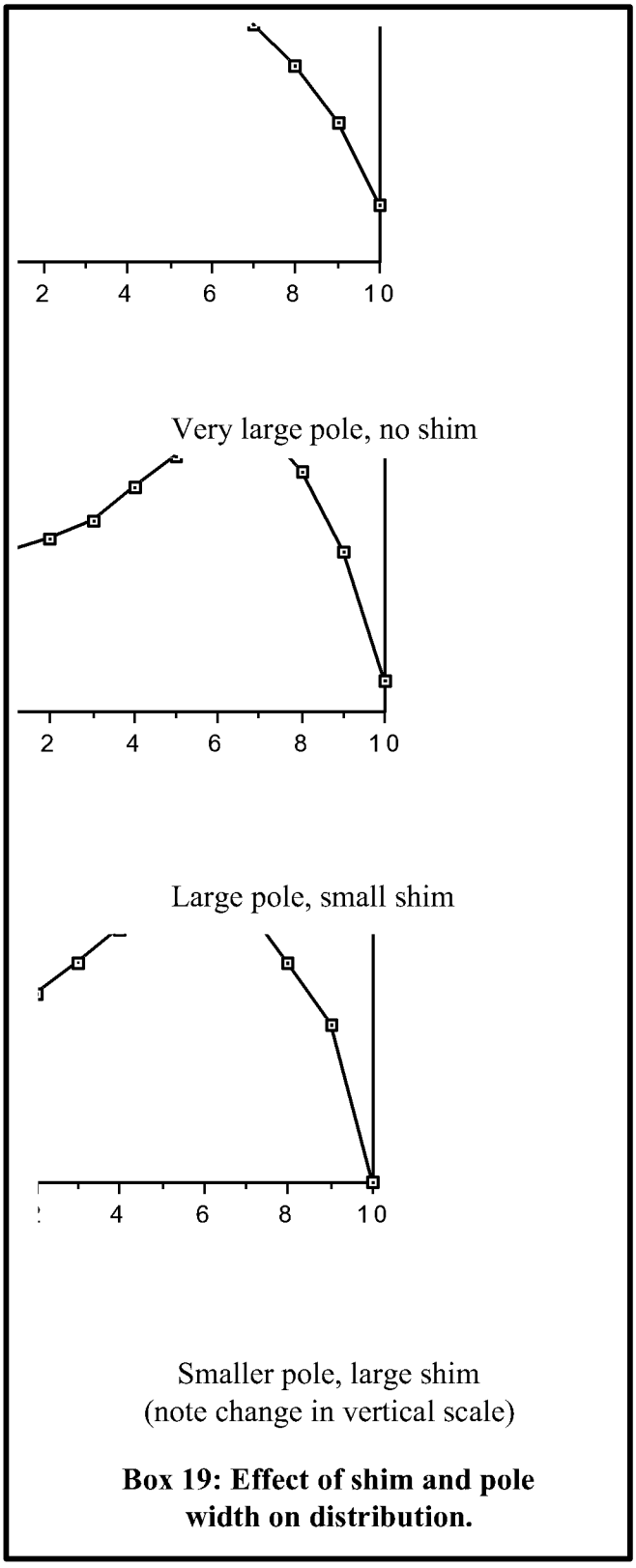

Box 19: Effect of shim and pole width on distribution.

In an attempt to steer the student who is new to the topic through this rather intuitive subject, the following brief notes are offered as a guide; they do not represent a definitive procedure for establishing a design:

i) Start with a small shim to explore the sensitivity of the distribution to the shim area. Use this to obtain a better estimate of the size of shim that you need. In a dipole, the shim height will normally be a few percent of the gap, extending over less than five percent of the pole face.

ii) Note that the above numbers are very dependent on the required field quality; very flat dipole fields (of the order of 1 part in 10^4) will need very low shims and a wide pole, whilst a bigger shim, which produces a significant rise in field at the pole edge before it falls off rapidly, can be used for lower quality fields. This will give a saving in pole width. The effects of pole width and shim size are described in Box 19.

iii) When near the optimum, make only small changes to shim height; for an accelerator dipole, with gaps typically between 40 and 60 mm, a 20μm change across the shim makes some difference when the field is close to optimum. This sensitivity gives a clear indication of the

dimensional tolerances that will be needed during magnet construction.

Dipole:	plot $(B_Y(x) - B_Y(0))/B_Y(0)$
Quad:	plot $dB_Y(x)/dx$
Sext:	plot $d^2B_Y(x)/dx^2$

Box 20: Judgement of field quality.

iv) In the case of a quadrupole, vary the point at which the tangent breaks from the pole; this of course will also vary the position of the corner of the pole. Make changes of 1 mm or less at the position of the tangent break; again, sensitivity to 20μm changes in the vertical position of the corner will alter the distribution for a typical accelerator quadrupole.

v) For a sextupole, the pole shaping is less critical; the ideal third-order curve would be expensive to manufacture and is not necessary. Start with a simple rectangular pole and make a linear cut symmetrically placed at each side of the pole. Optimise the depth and angle of this cut and it will usually be found to be adequate.

vi) When judging the quality of quadrupole and sextupole fields, examine the differentials, not the fields. When using numerical outputs from the simpler codes, take first or second differences. This is illustrated in Box 20.

vii) In all cases, check the final distribution at different levels of flux density, particularly full excitation. If there is a large change in distribution between low and high inductions (and these are unacceptable), the shims are too high. Start again with a slightly wider pole and a lower, broader shim.

viii) Steel-cored magnets are limited by saturation effects. In dipoles, this appears as an inability to achieve high values of flux density without using excessive currents. In the case of quadrupoles and sextupoles, saturation may also limit the extent of the good field region at full excitation. In this case, the only solution is to lengthen the magnet and reduce the gradient.

3.7 Field computation codes

A number of standard codes are available for the pole design process described above. Three well known packages are compared in Box 21. The first two are simpler, two-dimensional codes, and are ideal for those new to the subject.

MAGNET is a 'classical' two-dimensional magnetostatic code with a finite rectangular mesh, differential analysis and non-linear steel. Separate iterations for the air and steel regions are used to converge on the solution with permeabilities approximating to the physical situation. The first solution (cycle 0) uses infinite permeability in steel; this is then adjusted on subsequent cycles. Output is B_X and B_Y in air and steel for the complete model, plus plots of permeability in steel and vector potential in air (to give total fluxes) and (in one version) an harmonic analysis. It is quickly and easily learned but suffers from the lack of pre- and post-processing. This means that all input data is numerical and the complete geometry has to be worked out exactly in Cartesian coordinates before entering into the code. Likewise, the output is in terms of numerical flux densities (in Gauss) and any calculation of gradients etc must be carried out by hand calculation or by typing into another code. A potentially mis-

Advantages	Disadvantages:
MAGNET:	
* Quick to learn, simple to use; * Small(ish) cpu use; * Fast execution time;	* Only 2D predictions; * Batch processing only - slows down problem turn-round time; * Inflexible rectangular lattice; * Inflexible data input; * Geometry errors possible from interaction of input data with lattice; * No pre or post processing; * Poor performance in high saturation;
POISSON:	
* Similar computation as MAGNET; * Interactive input/output possible; * More input options with greater flexibility; * Flexible lattice eliminates geometery errors; * Better handing of local saturation; * Some post processing available.	* Harder to learn; * Only 2D predictions.
TOSCA:	
* Full three dimensional package; * Accurate prediction of distribution and strength in 3D; * Extensive pre/post-processing;	* Training course needed for familiarisation; * Expensive to purchase; * Large computer needed. * Large use of memory. * Cpu time is hours for non-linear 3D problem.

Box 21: Comparison of three commonly used magnet computation codes.

leading feature of MAGNET is the way the program interprets input data by registering boundaries only on the lines of the fixed rectangular mesh. This means that data containing points that are not on a mesh line in at least one plane can be seriously misinterpreted and the geometry used for the prediction will differ from that intended by the designer.

A number of different versions of POISSON now exist. They offer similar capability to MAGNET, but go a long way to overcoming the more major problems with that program. A flexible triangular lattice is used and this is 'relaxed' by the software to fit the geometry during the first stage of execution. This overcomes the data input problem outlined above, it allows a more complex set of input specifications to be used (linear and curved boundaries can be specified) and post-processing gives output graphs in the interactive versions. The triangular mesh can be concentrated into areas of high induction, resulting in better handling of saturation. It is still, however, two dimensional.

By comparison, TOSCA is a state-of-the-art, three dimensional package that is maintained and updated by a commercial organisation in U.K. The software suite is available from this company, and training courses are offered to accustom both beginners and more experienced designers to the wide range of facilities available in the program.

There are now a large number of field computation packages available for both accelerator and more general electrical engineering purposes. The decision not to mention a certain package in this paper does not imply any criticism or rejection of that program. The three chosen for description are, however, 'classic' packages that perhaps represent three separate stages in the development of the computation program.

It should not be believed that the lack of three-dimensional information in the simpler packages prevents the designer obtaining useful information concerning the magnet in the azimuthal direction. The next two sections will therefore deal with the topic of magnet ends and how they are addressed numerically.

3.8 Magnet ends

Unless the magnet is playing a relatively unimportant role in the accelerator, the magnet designer must pay particular attention to the processes that are occurring at the magnet ends. The situation is summarised in Box 22. A square end (viewed in the longitudinal direction) will collect a large amount of flux from the fringe region and saturation may occur. Such a sharp termination also allows no control of the radial field in the fringe region and produces a poor quality distribution. This fringe area will normally contribute appreciably to the integrated field seen by the beam, the actual percentage depending on the length of the magnet. It is quite pointless to carefully design a pole to give a very flat distribution in the centre of the magnet if the end fields totally ruin this high quality. The end distribution, in both the longitudinal and transverse planes, must therefore be controlled.

Square ends:

* display non linear effects (saturation);
* give no control of radial distribution in the fringe region.

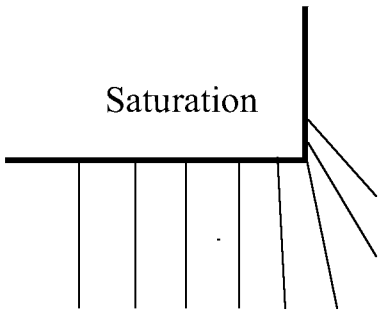

Chamfered ends:

* define magnetic length more precisely;
* prevent saturation;
* control transverse distribution;
* prevent flux entering iron normal to lamination (vital for ac magnets).

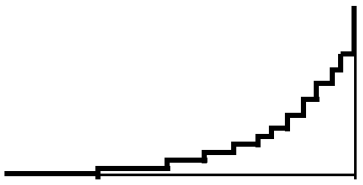

Box 22: Control of longitudinal field distributions in magnet ends.

This is usually achieved by 'chamfering' or 'rolling off' the magnet end, as shown in Box 22. A number of standard algorithms have been described for this, but the exact shape is of no great importance except in very high flux density magnets. The important criteria for the roll off are:

i) It should prevent appreciable non-linear (saturation) effects at the ends for all levels of induction.

ii) It should provide the designer with control of transverse distribution throughout the region where the fringe flux is contributing appreciably to the magnet strength.

iii) It should not occupy an uneconomically large region.

iv) It should, in a.c. applications, prevent appreciable flux entering normal to the plane of the laminations.

Dipole:

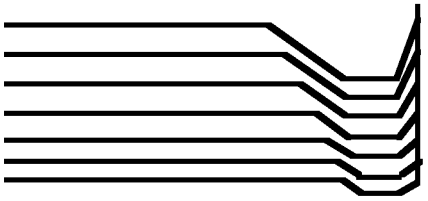

Quadrupole:

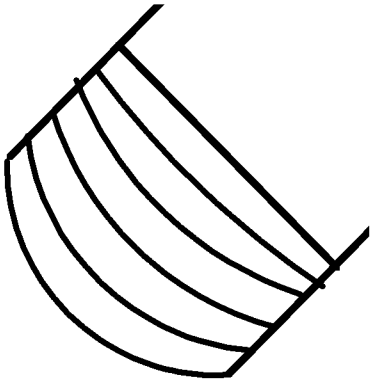

Box 23: Contol of transverse distribution in end regions with non-standard poles.

Looking at these chamfered end regions in the transverse plane again, it is then the practice to profile the magnet pole to attempt to maintain good field quality as the gap increases and the flux density reduces. Box 23 describes the typical geometries that are used. In the case of the dipole, the shim is increased in size as the gap gets larger; for the quadrupole the pole shape is approximated to the arcs of circles with increasing radii. It should be appreciated that such techniques cannot give ideal results, for it must be assumed that the pole width was optimised for a given gap dimension. Hence, no shim will be found that can give a good field distribution with the same pole width and larger gap. However, the fringe region will only contribute a certain percentage to the overall field integral and hence the specification can be degraded in this region. In some cases, integrated errors in the end region can be compensated by small adjustments to the central distribution; however, to use this technique, the designer must be particularly confident of the end-field calculations.

3.9 Calculation of end field distributions

Even using two-dimensional codes, numerical estimates of the flux distribution in the magnet ends can be made. The use of an idealised geometry to estimate the longitudinal situation in a dipole is shown in Box 24. The right hand side of the model approximates to the physical magnet, with the end roll-off and the coil in the correct physical positions. However, the return yoke and the coil on the left are non-physical abstractions; they are needed to provide the magnetomotive force and a return path for the flux in the two dimensional model. Thus the flux distribution in the end region will be a good representation of what would be expected on the radial centre plane of the magnet. This model can therefore be used to check the field roll off distribution, the

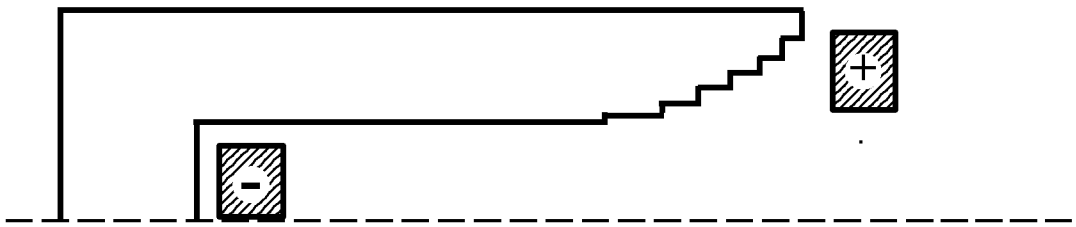

The diagram shows an idealised geometry in the longitudinal plane of a dipole, as used to estimate end-field distributions. The right hand coil is at the correct physical position; the coil and return yoke on the left are idealised to provide excitation and a return path for the flux in two dimensions.

Box 24: Calculation of longitudinal end effects using two-dimensional codes.

flux density at the steel surface in the chamfer, and the expected integrated field length of the magnet; this last parameter is, of course, of primary importance as it determines the strength of the magnet.

In the case of the quadrupole, the similar calculation is less useful. The same model can be used, taking a section through the 45 line, ie on the inscribed radius, but this will look like a dipole and predict a non-zero field at the magnet centre. The only useful feature will therefore be an examination of the flux densities at the steel surface in the end regions by normalising to the value predicted for the central region in the transverse calculations. As saturation on the pole is seldom encountered in a quadrupole (if present, it is usually in the root of the pole), this is of little value.

It is not usually necessary to chamfer the ends of sextupoles; a square cut off can be used.

Turning now to the transverse plane in the end region, it is quite practical to make calculations with the increased pole gap and enlarged shim for each transverse 'slice' through the end. The shim can be worked on to optimise the field distribution as best as possible, and the prediction of transverse distribution used with some confidence. However, the predicted amplitude of flux density will be incorrect, for there will be a non-zero field derivative in the plane normal to the two-dimensional model. In principle, the distribution is also invalidated by this term, but experience indicates that this is a small effect. Hence, the designer must normalise the amplitude of the flux density in each 'slice' to that predicted in the longitudinal model. The resulting normalised distributions can then be numerically integrated (by hand calculation!) and added to the integrated radial distribution in the body of the magnet. This gives a set of figures for the variation of integrated field as a function of radial position - the principal aim of the whole exercise. Of course, all this can be avoided if a full three-dimensional program is used and the complete magnet will be computed in one single execution. However, the above procedure gives a very satisfactory prediction if an advanced code is not available; it also gives the designer a good 'feel' for the magnet that is being worked upon.

3.10 Magnet manufacture

This is a specialised topic, the details of which are perhaps best left to the various manufacturers that make their living by supplying accelerator laboratories. However, a few comments should help the designer when preparing for this exercise.

For d.c. accelerator magnets, yokes are usually laminated. This allows the 'shuffling' of steel to randomise the magnetic properties. Laminations also prevent eddy current effects which, even in d.c. magnets, can cause problems with decay time constants of the order of minutes. Laminations are therefore be regarded as essential in storage rings which are ramped between injection and full energy.

The laminations are 'stamped' using a 'stamping tool'. This must have very high precision and reproducibility (~20μm). Manufacturers involved in standard electrical engineering production will regard this figure as stringent but possible. The dimensions of the lamination must be checked on an optical microscope every five to eight thousand laminations.

Assembly of the laminations is in a fixture; the number of laminations in each stack is determined by weight and hydraulic pressure is used to define the length. At one time, the stacked laminations were glued together, but now it is more usual to weld externally whilst the stack is firmly held in the fixture. If a.c. magnets are being assembled the welding must not produce shorted turns.

Coils are wound using glass insulation wrapped onto the copper or aluminium conductor before receiving an 'outerground' insulation of (thicker) glass cloth. The assembly is then placed in a mould and heated under vacuum to dry and outgas. The mould is subsequently flooded with liquid epoxy resin that has been mixed with the catalyst under vacuum. The vacuum tank is let up to atmosphere, forcing the resin deep into the coil to produce full impregnation. 'Curing' of the resin then occurs at high temperature. Total cleanliness is essential during all stages of this process!

Rigorous testing of coils, including water pressure, water flow, thermal cycling and 'flash' testing at high voltage whilst the body of the coil is immersed in water (terminals only clear) is strongly recommended. This will pay dividends in reliability of the magnets in the operational environment of the accelerator.

BIBLIOGRAPHY

Many text-books provide a sound theoretical description of fundamental magneto-statics as described in this paper, but for a clear and easily understood presentation see:

B.I. Bleaney and B. Bleaney, Electricity and Magnetism, (Oxford University Press, 1959)

For a more advanced presentation, see:

W.K.H. Panofsky and M. Phillips, Classical Electricity and Magnetism, (Addison - Wesley Publishing Co., 1956).

Many magnet designs for accelerator applications have been described in detail in the series of International Conferences on Magnet Technology. Given below are the dates and venues of these conferences; the proceedings of these Conferences provide many examples of d.c, a.c. and pulsed magnet design:

1965 Stanford Ca, USA;
1967 Oxford, UK;
1970 Hamburg, Germany;
1972 Brookhaven N.Y., USA;
1975 Rome, Italy;
1977 Bratislava, Czechoslovakia
1981 Karlsruhe, Germany;
1983 Grenoble, France;
1985 Zurich, Switzerland;
1989 Boston, USA.